Corrections

BIOCHEMISTRY

Correction for "CRL4-like Clr4 complex in *Schizosaccharomyces pombe* depends on an exposed surface of Dos1 for heterochromatin silencing," by Canan Kuscu, Mikel Zaratiegui, Hyun Soo Kim, David A. Wah, Robert A. Martienssen, Thomas Schalch, and Leemor Joshua-Tor, which appeared in issue 5, February 4, 2014, of *Proc Natl Acad Sci USA* (111:1795–1800; first published January 21, 2014; 10.1073/pnas.1313096111).

The authors note that Fig. 2 and its corresponding legend appeared incorrectly. The corrected figure and its corrected legend appear below. In addition, the authors note that on page 1797, right column, last paragraph, Fig. 2*C* should appear as Fig. 2*B*.

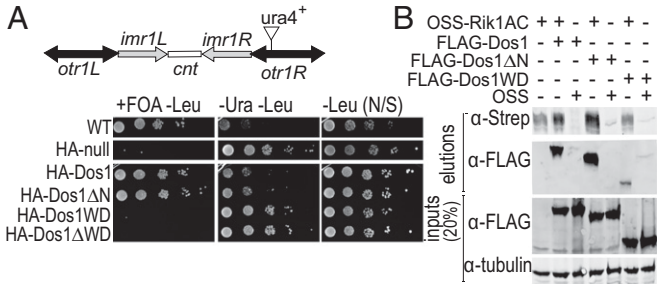

Fig. 2. The WD40 repeat domain of Dos1 is essential but not sufficient for heterochromatin formation at the *S. pombe* centromere. (*A*) Schematic diagram of *S. pombe* centromere 1. The position of the centromeric *otr1R::ura4* reporter insertion used in this study is indicated. Comparative growth assay of the serially diluted *dos1* null strain with the centromeric *otr1R::ura4* reporter expressing the indicated Dos1 fragments from a plasmid. Strains were examined for growth on pombe glutamate media (PMG) lacking leucine and supplemented with 1 g/L 5-FOA (+FOA –Leu), PMG media lacking uracil and leucine (–Ura –Leu), and PMG media lacking leucine (–Leu). Cells were always grown on a PMG medium lacking leucine to select for Dos1 expressing plasmid. (*B*) OSS-Rik1AC was coexpressed with FLAG-Dos1 truncations and pulled down with Strep-Tactin beads to detect whether the interactions are still preserved in Dos1 truncations.

www.pnas.org/cgi/doi/10.1073/pnas.1417135111

NEUROSCIENCE

Correction for "Manganese-enhanced magnetic resonance imaging reveals increased DOI-induced brain activity in a mouse model of schizophrenia," by Natalia V. Malkova, Joseph J. Gallagher, Collin Z. Yu, Russell E. Jacobs, and Paul H. Patterson, which appeared in issue 24, June 17, 2014, of *Proc Natl Acad Sci USA* (111:E2492–E2500; first published June 2, 2014; 10.1073/pnas.1323287111).

The authors note that in all experiments, the concentration for $MnCl_2$ should be 0.4 mmole/kg body weight instead of 40 mmole/kg body weight. The incorrect text appears on page E2493, Fig. 2 legend, lines 1, 2, and 5; on page E2494, Fig. 4 legend, line 3; on page E2494, left column, first full paragraph, line 10; and on page E2498, right column, fourth full paragraph, lines 3 and 4. This error does not affect the conclusions of the article.

www.pnas.org/cgi/doi/10.1073/pnas.1416478111

NEUROSCIENCE

Correction for "Hippocampal damage impairs recognition memory broadly, affecting both parameters in two prominent models of memory," by Adam J. O. Dede, John T. Wixted, Ramona O. Hopkins, and Larry R. Squire, which appeared in issue 16, April 16, 2013, of *Proc Natl Acad Sci USA* (110:6577–6582; first published April 1, 2013; 10.1073/pnas.1304739110).

The authors note that the following statement should be added as a new Acknowledgments section: "We thank Jennifer Frascino and Erin Light for assistance. This work was supported by the Medical Research Service of the Department of Veteran Affairs and National Institute of Mental Health Grant MH24600."

www.pnas.org/cgi/doi/10.1073/pnas.1417124111

Correction for "Kaposi's sarcoma-associated herpesvirus LANA recruits the DNA polymerase clamp loader to mediate efficient replication and virus persistence," by Qiming Sun, Toshiki Tsurimoto, Franceline Juillard, Lin Li, Shijun Li, Erika De León Vázquez, She Chen, and Kenneth Kaye, which appeared in issue 32, August 12, 2014, of *Proc Natl Acad Sci USA* (111:11816–11821; first published July 28, 2014; 10.1073/pnas.1404219111).

The authors note that Fig. 3 appeared incorrectly. The corrected figure and its legend appear below.

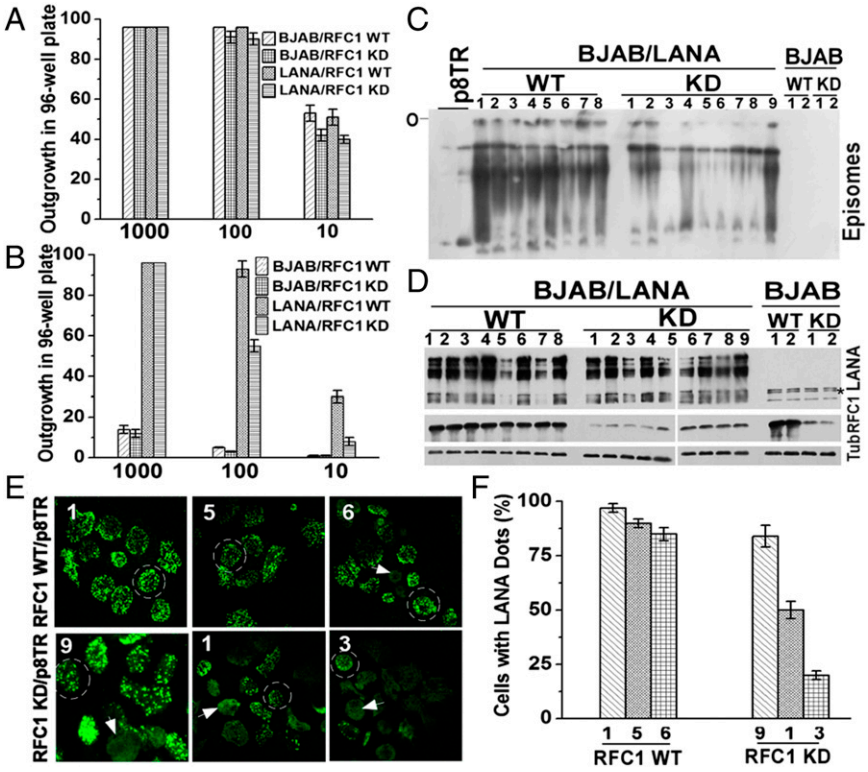

Fig. 3. LANA interaction with RFC is critical for LANA-mediated episome persistence. (*A*) BJAB or BJAB/LANA outgrowth in microtiter plates after seeding at 1,000, 100, or 10 cells per well in the presence or absence of RFC1 knockdown (KD). Averages of three experiments are shown. Error bars indicate SD. (*B*) G418-resistant outgrowth of BJAB or BJAB/LANA cells after p8TR transfection with or without RFC1 knockdown. Averages of three experiments, with SD, are shown. (*C*) Gardella gel analysis (27) assessing the presence of episomal DNA in BJAB or BJAB/LANA cells with or without RFC1 KD after 20 d of G418 selection. Numbers refer to independently derived G418-resistant cell lines expanded from individual microtiter wells. The two leftmost lanes have increasing amounts of naked p8TR plasmid. O, gel origin. (*D*) Western blot analysis for LANA, RFC1, or Tub in cell lines used for Gardella gel analysis (27) in *C*. The asterisk indicates nonspecific bands. (*E*) LANA immunostaining in the indicated cell lines from *C* with or without RFC1 KD. Cell lines 1, 5, and 6 (WT, *Upper*) or cell lines 9, 1, and 3 (RFC1 KD, *Lower*) contain successively lower levels of episomal DNA as observed in *C*. Broad nuclear LANA staining indicates episome loss (arrowheads), whereas LANA dots (circled cells) indicate sites of episomes. (Magnification: 630×.) (*F*) Quantification of average percentage of cells containing LANA dots. Averages of three experiments, with SD, are shown.

www.pnas.org/cgi/doi/10.1073/pnas.1416630111

Manganese-enhanced magnetic resonance imaging reveals increased DOI-induced brain activity in a mouse model of schizophrenia

Natalia V. Malkova[a,1], Joseph J. Gallagher[a], Collin Z. Yu[b], Russell E. Jacobs[a], and Paul H. Patterson[a]

[a]Division of Biology and Biological Engineering, California Institute of Technology, Pasadena, CA 91125; and [b]School of Pharmacy, University of California, San Francisco, CA 94143-0622

Edited by Terrence J. Sejnowski, Salk Institute for Biological Studies, La Jolla, CA, and approved May 5, 2014 (received for review December 18, 2013)

Maternal infection during pregnancy increases the risk for schizophrenia in offspring. In rodent models, maternal immune activation (MIA) yields offspring with schizophrenia-like behaviors. None of these behaviors are, however, specific to schizophrenia. The presence of hallucinations is a key diagnostic symptom of schizophrenia. In mice, this symptom can be defined as brain activation in the absence of external stimuli, which can be mimicked by administration of hallucinogens. We find that, compared with controls, adult MIA offspring display an increased stereotypical behavioral response to the hallucinogen 2,5-dimethoxy-4-iodoamphetamine (DOI), an agonist for serotonin receptor 2A (5-HT2AR). This may be explained by increased levels of 5-HT2AR and downstream signaling molecules in unstimulated MIA prefrontal cortex (PFC). Using manganese-enhanced magnetic resonance imaging to identify neuronal activation elicited by DOI administration, we find that, compared with controls, MIA offspring exhibit a greater manganese (Mn^{2+}) accumulation in several brain areas, including the PFC, thalamus, and striatum. The parafascicular thalamic nucleus, which plays the role in the pathogenesis of hallucinations, is activated by DOI in MIA offspring only. Additionally, compared with controls, MIA offspring demonstrate higher DOI-induced expression of early growth response protein 1, cyclooxygenase-2, and brain-derived neurotrophic factor in the PFC. Chronic treatment with the 5-HT2AR antagonist ketanserin reduces DOI-induced head twitching in MIA offspring. Thus, the MIA mouse model can be successfully used to investigate activity induced by DOI in awake, behaving mice. Moreover, manganese-enhanced magnetic resonance imaging is a useful, noninvasive method for accurately measuring this type of activity.

polyinosinic:polycytidylic acid | neurodevelopment | MEMRI | immediate early gene

Although it is possible to assay traits in animal models that are similar to those found in human schizophrenia, these traits are also found in animal models of other neurodevelopmental disorders such as autism spectrum disorder (ASD) (1, 2). According to the *Diagnostic and Statistical Manual of Mental Disorders, Fifth Edition*, hallucinations represent one such hallmark characteristic of schizophrenia but not of ASD. In humans, serotonin receptor 2A (5-HT2AR) agonists, such as lysergic acid diethylamide (LSD), mescaline, psilocybin, and 2,5-dimethoxy-4-iodoamphetamine (DOI), can trigger effects similar to the positive symptoms of schizophrenia such as delusions and hallucinations (3, 4). Moreover, use of drugs plays a precipitating role in the development of earlier onset of psychosis among schizophrenic patients (5). We are investigating 5-HT2AR activation in a mouse model of an environmental risk factor for schizophrenia and autism, maternal immune activation (MIA). Offspring of infected or immune-activated pregnant mice and rats exhibit a number of features associated with schizophrenia including deficits in sensorimotor gating, latent inhibition and social interaction, increased dopamine turnover and responsiveness, enhanced sensitivity to amphetamine and MK-801, and ventricular enlargement. Moreover, several of these behavioral abnormalities are adult-onset and reversed by antipsychotic medications (6–8).

To study DOI-induced activity in MIA offspring, we developed an approach using manganese-enhanced magnetic resonance imaging (MEMRI). By taking advantage of the fact that Mn^{2+} enters excitable cells via voltage-gated calcium channels, MEMRI has been used to study cocaine-induced neuronal activity (9), brain plasticity in song birds (10), and sound-evoked activity (11, 12). The approach in the first two studies has some limitations, as it is invasive, whereas the latter study required exposure to a prolonged, repetitive stimulus. We developed a noninvasive method to map brain regions of DOI-induced activity in awake, behaving mice. Our approach decouples isofluorane anesthesia, which is necessary for image acquisition, from DOI administration and behavioral and brain responses to the drug. We then used this method to analyze DOI-induced brain activity in MIA and control offspring.

We next confirmed MEMRI data using immediate early gene (IEG) induction as a surrogate of neuronal activity and investigated the effects of MIA on the expression of 5-HT2AR and its downstream signaling molecules. Our data demonstrate that DOI-induced hallucination-like activity can be modeled in the MIA mouse model and MEMRI can be successfully used to measure this kind of activity.

Significance

Here, we model a positive symptom of schizophrenia, hallucination-like activity, in a mouse model of an environmental risk factor of schizophrenia, maternal immune activation (MIA). MIA offspring display an enhanced susceptibility to the hallucinogen 2,5-dimethoxy-4-iodoamphetamine (DOI) and demonstrate elevated DOI-induced brain activity as measured by induction of immediate early genes and manganese-enhanced MRI. High sensitivity to DOI in MIA offspring can be explained by an increased level of serotonin receptor 2A (5-HT2AR) that mediates the effect of DOI on the prefrontal cortex. Chronic treatment with the 5-HT2AR antagonist ketanserin reduces DOI-induction of head twitching in MIA offspring. Our data demonstrate that DOI-induced hallucination-like activity can be modeled in the MIA mouse model and suggest 5-HT2AR as a potential therapeutic target for schizophrenia.

Author contributions: N.V.M. and P.H.P. designed research; N.V.M. and J.J.G. performed research; N.V.M., J.J.G., C.Z.Y., and R.E.J. analyzed data; and N.V.M., J.J.G., R.E.J., and P.H.P. wrote the paper.

The authors declare no conflict of interest.

This article is a PNAS Direct Submission.

[1]To whom correspondence should be addressed. E-mail: malkova@caltech.edu.

This article contains supporting information online at www.pnas.org/lookup/suppl/doi:10.1073/pnas.1323287111/-/DCSupplemental.

www.pnas.org/cgi/doi/10.1073/pnas.1323287111

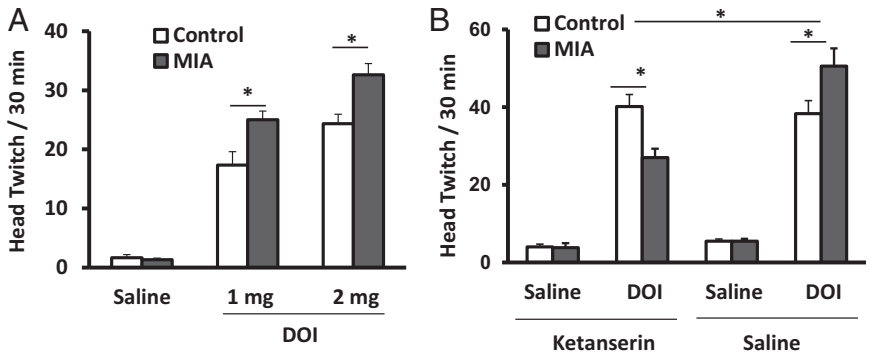

Fig. 1. DOI induces dose-dependent stereotypic behavior that is blocked by ketanserin. Compared with controls, MIA offspring display more head twitching (*A*) in response to DOI ($n = 9$–13 from three to four litters per group, $^*P < 0.05$). (*B*) Chronic blockade of 5-HT2Rs was achieved by daily injections of ketanserin (2 mg/kg) i.p. for a week. Two days after the last injection, animals were treated with DOI (1 mg/kg) or saline, and the behavioral responses recorded for 30 min ($n = 6$–7 from three litters in DOI-treated groups with or without ketanserin; $n = 4$–5 from three litters in saline-treated groups with or without ketanserin, $^*P < 0.05$). Data are presented as mean ± SEM.

Results

Compared with Control Offspring, MIA Offspring Exhibit Increased Stereotypical Behavioral Responses to DOI. Drug-induced head twitches are characteristic of animals exposed to hallucinogens, and these are positively correlated with drug-induced hallucinations in humans (13–15). DOI-induced head twitches are elicited by activation of 5-HT2ARs in the prefrontal cortex (PFC) (14, 16, 17). We find that DOI induces this behavior in MIA and control mice in a dose-dependent manner [$F_{(1,\ 28)} = 75.6$, $P < 0.0001$ and $F_{(1,\ 33)} = 116.4$, $P < 0.0001$ for 1 and 2 mg/kg DOI, respectively; post hoc tests, $P < 0.001$ for both 1 and 2 mg/kg DOI for control and MIA offspring] (Fig. 1*A*). However, compared with controls, MIA offspring display a significantly greater response [for 1 mg/kg DOI, $F_{(1,\ 28)} = 3.884$, $P = 0.059$; post hoc test, $P < 0.05$; for 2 mg/kg DOI, $F_{(1,\ 33)} = 3.56$, $P = 0.068$; post hoc test, $P < 0.01$].

Single i.p. Injection of $MnCl_2$ Has No Significant Effect on General Mouse Health and DOI-Induced Behavior and Brain Activity. Functional magnetic resonance imaging (fMRI) is one of the most widely used noninvasive neuroimaging methods that measure functional brain activity in rodents (18). Our attempt to assess global neural responses to DOI using a typical fMRI protocol (18) was not successful. Possible explanations include a robust

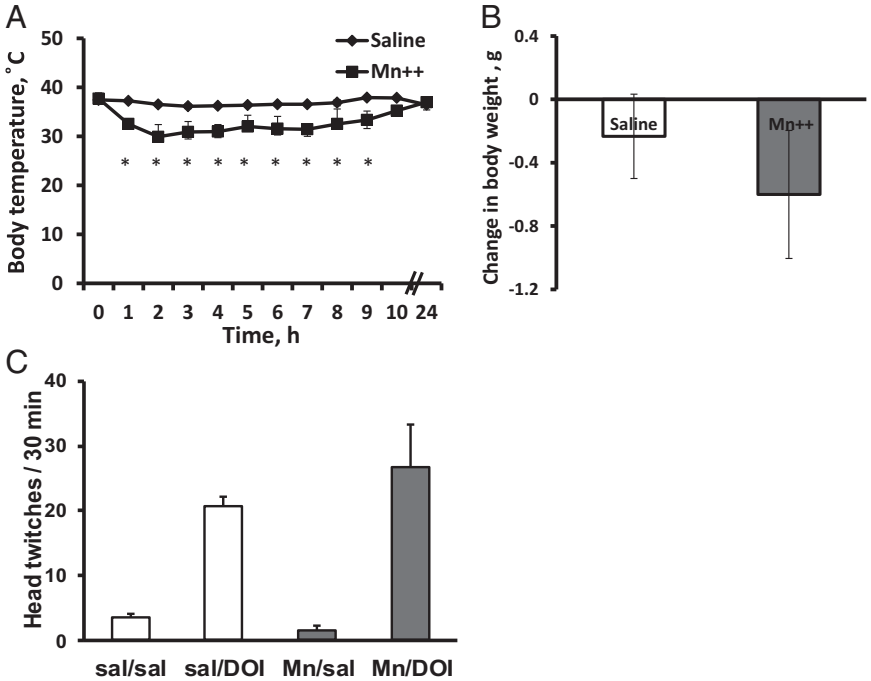

Fig. 2. Effect of intraperinoneal injection of $MnCl_2$ on mouse general health and DOI-induced head twitching. (*A*) Mice treated with $MnCl_2$ (40 mmole/kg body weight) displayed a dramatic decrease in the body temperature during first the 10 h after injection [$F_{(1,\ 48)} = 159.9$, $^*P < 0.0001$]. The mean baseline temperature for the mice before $MnCl_2$ exposure was 37.6 ± 0.1 °C. (*B*) Mice injected with $MnCl_2$ maintain their body weight 24 h after injection [$t_{(4)} = 0.922$, $P = 0.419$]. To determine change in body weight, initial body weight was subtracted from body weight 24 h after injection. (*C*) $MnCl_2$ has no significant effect on DOI-induced behavioral response. Mice obtained $MnCl_2$ injection i.p. (40 mmole/kg body weight) 24 h before behavior testing. On the day of the test, animals were injected with 2 mg/kg DOI or saline, and their behavior was monitored for 30 min. Injections of $MnCl_2$ did not affect DOI-induced head twitching [$F_{(1,\ 8)} = 0.533$, $P = 0.486$]. Data represent means ± SEM; $n = 3$ mice per treatment group.

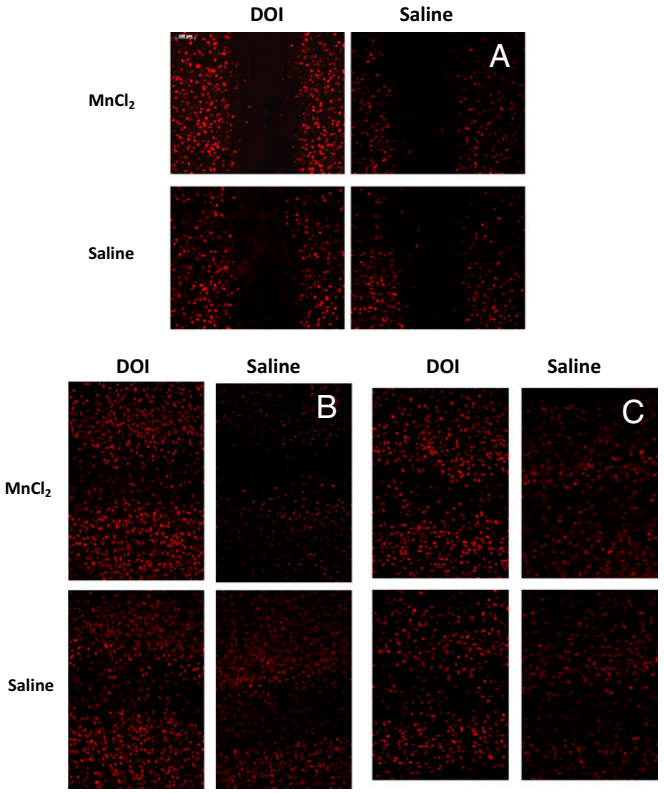

Fig. 3. $MnCl_2$ has no significant effect on DOI-induced activation of IEG *egr1*. Sensory cortices sampled are frontal (*A*), somatosensory (*B*), and auditory (*C*).

cardiovascular effect of DOI (19) due to the presence of 5-HT2AR within the vasculature (20). Moreover, even under isofluorane anesthesia, the drug-induced body jerks and head twitches make imaging extremely difficult. Isofluorane anesthesia also blocked DOI-induced IEG early growth response protein 1 (egr-1) response (Fig. S1).

Therefore, to track brain activity in awake, freely moving animals, we used a modified MEMRI protocol that decouples isofluorane anesthesia and DOI administration. Previously, MEMRI was successfully applied to analyze cocaine-, sound-, and odor-induced activities (9, 11, 12, 21), as well as brain plasticity in song birds (10). Because Mn^{2+} can be neurotoxic (22, 23), we carried out a pilot experiment on naive, 6-wk-old C57BL/6J mice to establish a protocol and study the effects of Mn^{2+} on general animal health and DOI-induced behavior. We found that Mn^{2+} ($MnCl_2$, 40 mmole/kg body weight) decreases body temperature during the first 10 h (Fig. 2*A*). By 12 h, the body temperature was 36.97 ± 0.19 °C. To stabilize the body temperature, we kept animals on a heating pad during this time. With this precaution, no significant effects of Mn^{2+} on body weight, DOI-induced head twitching, or egr-1 activation were found (Figs. 2 *B* and *C* and 3). The animals also received an i.p. injection of saline (300 μL per mouse) 3 and 6 h after $MnCl_2$ injection to keep them hydrated.

MIA Offspring Display Greater DOI-Induced Brain Activation as Detected by MEMRI. To track brain activity in awake, freely moving animals, we used a modified MEMRI protocol, in which neuronal activity is imaged retrospectively, after DOI-induced Mn^{2+} accumulation within activated neurons of awake, behaving mice (Fig. 4). For the analysis, we apply an MEMRI-based statistical parametric mapping (SPM) method that was successfully used to measure sound-induced activity in a quantitative and unbiased manner (9, 12). We compare DOI-induced Mn^{2+} uptake in MIA versus control offspring performing a 2 × 2 factorial analysis with drug (DOI or saline) and MIA [poly(I:C) or saline] treatments as the independent factors and the signal intensity difference before and after drug administration as the dependent factor. Significant Drug × Group interactions are identified, and these are overlaid onto a study-specific minimum deformation template (MDT) and presented as statistical parametric *F*-value maps (Fig. 5 and Table S1). The green color represents areas with the cumulative effect of DOI in MIA and control mice (Fig. 5, *Right*). A DOI effect is observed throughout the brain, predominately in somatosensory cortices and regions associated with motor function, often with lateralization to a specific hemisphere. The primary motor area (layer 6a), secondary motor area (layers 2, 3, and 5), primary somatosensory area for the upper and lower limb, and caudate putamen all display increased Mn^{2+} accumulation, with distinct lateralization in the left hemisphere. An increase is also observed in the orbital area; layers 1, 2, and 3 of the infralimbic area; the dorsal part of the anterior cingulate; and the dorsal portion of the taenia tecta layer 1. Bilateral increases are observed in the medial group of the dorsal thalamus. Then, direct comparison of the increases due to DOI in the MIA and control groups was performed for the voxels that demonstrate statistically significant interaction effects in 2 × 2 factorial analysis (Fig. 6*A* and Table S2; Student *t* test, $P < 0.05$). Here, red indicates that the DOI response is significantly greater in MIA compared with the control offspring; with blue representing the reverse (Fig. 6*B*). The difference between MIA and control offspring in response to DOI is observed in most of the areas described above. The parafascicular thalamic nucleus (PTN) is found to be activated by DOI in MIA offspring only. Compared with MIA offspring, the control mice exhibit increased DOI responses in very few brain areas. At this level of significance, no difference is found between the signal difference from 24 and 27 h in MIA and control offspring who received saline instead of DOI.

MIA Offspring Display Greater DOI-Induced egr-1, COX-2, and BDNF Activation in the PFC than Control Offspring. The PFC plays a key role in the control of DOI-induced head twitch behavior. Microinjections of DOI in the PFC elicit this type of stereotyped response in rodents (16). Moreover, restoration of 5-HT2AR in the PFC of 5-HT2AR knockout mice is sufficient to mediate DOI-induced activation of *egr-1* as well as behavioral responses (14). DOI also stimulates local 5-HT release, particularly in the PFC (24). Because MIA offspring display elevated sensitivity to DOI and increased Mn^{2+} accumulation in PFC as measured by MEMRI, we analyzed DOI-induced activation of *egr-1* in this part of the brain. We find that 1 mg/kg of DOI significantly increases egr-1 mRNA production

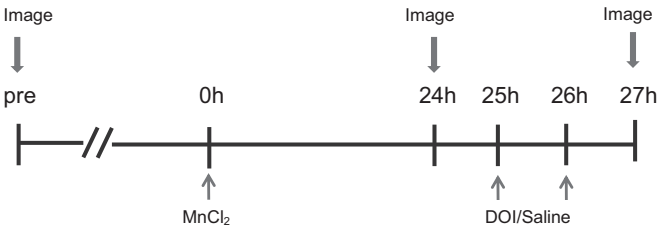

Fig. 4. The MEMRI experimental timeline is illustrated. Animals first underwent a 46-min baseline scan a week before the beginning of the experiment. On the first day, $MnCl_2$ (40 mmole/kg body weight) was delivered i.p., and 24 h later, the animals were imaged to measure the basal level of Mn^{2+} uptake in the brain. After recovery from anesthesia, the animals received two injections of DOI (2 mg/kg) or saline 1 h apart and were imaged again 1 h after the last DOI injection. All imaging scans were done under 2% isoflurane anesthesia.

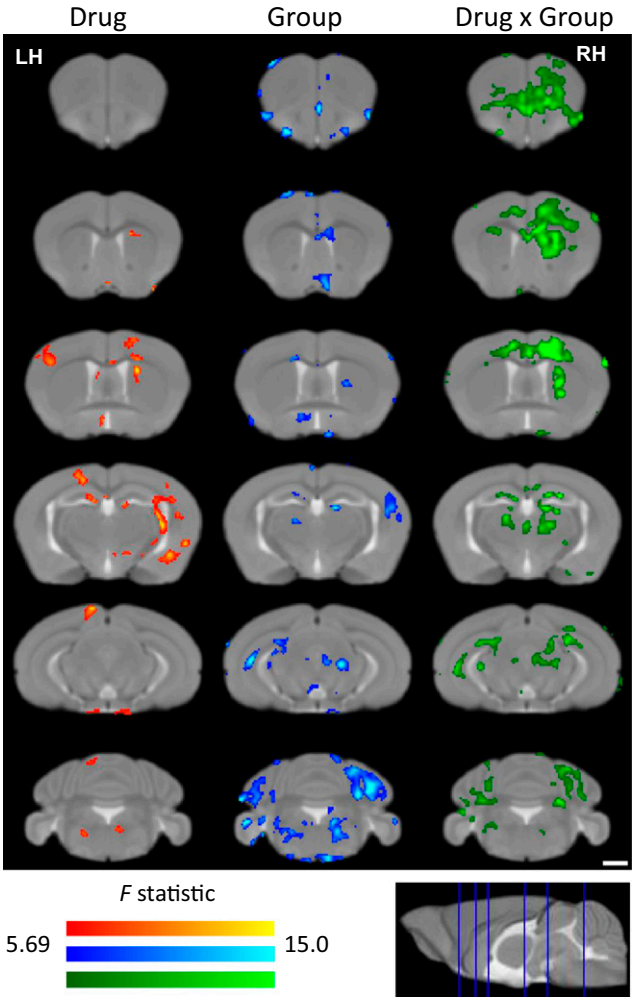

Fig. 5. Statistical parametric maps of DOI-induced MEMRI signal in MIA and control mice. MEMRI images were analyzed via voxel-by-voxel statistical comparisons. Multifactorial analysis (2 × 2) for Drug × Group interaction was performed. Drug (DOI or vehicle; red), group (MIA or control mice; blue), and Drug × Group interaction (green) *F* statistical maps are overlaid on coronal sections from a study-specific MDT. Corrections for multiple comparison effects were calculated using Alphasim, and significance was reached at $P < 0.0001$, with a minimum cluster size of 36 voxels corresponding to $\alpha = 0.01$; $n = 6$ per group. (Scale bar, 1 mm.) LH, left hemisphere; RH, right hemisphere.

in both groups [$F_{(1, 37)} = 34.4$, $P < 0.0001$; post hoc test, $P < 0.05$ for control mice and $P < 0.001$ for MIA offspring], but MIA offspring display higher DOI-induced *egr-1* activation in the PFC than controls. The post hoc test of differences in response to DOI reveals a significantly elevated egr-1 level in MIA offspring (MIA twofold increase versus control 1.5-fold increase, $P < 0.05$) (Fig. 7*A*).

DOI alters cyclooxygenase-2 (COX-2) expression, the key enzyme in the synthesis of prostaglandins, in the rat parietal cortex via stimulation of the PLA_2 pathway (25). We find that although the drug significantly increases COX-2 mRNA in both groups [$F_{(1, 41)} = 13.37$, $P < 0.001$; post hoc test, $P < 0.05$ for control mice and $P < 0.01$ for MIA offspring], MIA offspring display a threefold increase in COX-2 induction in the PFC compared with a 1.5-fold increase in controls [$F_{(1, 41)} = 6.068$, $P < 0.05$; post hoc test, $P < 0.05$] (Fig. 7*B*).

The level of the neurotrophin brain-derived neurotrophic factor (BDNF) is altered in schizophrenia (26), and DOI regulates its expression in the hippocampus and neocortex (27). We find that DOI increases BDNF mRNA in both MIA and control groups [$F_{(1, 36)} = 8.19$, $P < 0.01$; post hoc test, $P < 0.02$ for control mice and $P = 0.17$ for MIA offspring). However, MIA offspring display significantly higher DOI-induced BDNF mRNA expression in the PFC than controls [$F_{(1, 36)} = 8.63$, $P < 0.01$; post hoc test, $P < 0.05$] (Fig. 7*C*).

MIA Offspring Have an Increased Level of 5-HT2AR and Its Downstream Signaling Molecules in the PFC. Compared with controls, antipsychotic-free human schizophrenic subjects display an increased 5-HT2AR level in the PFC (28). Moreover, rodent models of schizophrenia, including MIA and prenatal or postnatal stress, yield offspring with elevated 5-HT2AR in the PFC, as well as a greater sensitivity to DOI (29–31). We find that, compared with controls, MIA offspring exhibit a 50% increase in 5-HT2AR mRNA levels in the PFC [$t_{(26)} = 2.738$, $P < 0.05$] (Fig. 7*D*). Moreover, MIA offspring display elevated mRNA levels for phospholipase C (PLC) β1 and regulator of G protein signaling 4 (RGS4), which are regulated by 5-HT2AR [$t_{(23)} = 3.301$, $P < 0.005$ and $t_{(22)} = 2.64$, $P < 0.05$ for PLC β1 and RGS4, respectively]. No difference between MIA and control offspring is seen for cytoplasmic phospholipase A_2 ($cPLA_2$) [$t_{(19)} = 0.1299$, $P = 0.898$], serotonin transporter (SERT) [$t_{(20)} = 0.085$, $P = 0.933$], and integrin β 3 (ITGB3) [$t_{(20)} = 0.417$, $P = 0.682$]. Moreover, we find that 5-HT2AR and PLC β1, but not RGS4, exhibit trending increases at the protein level, consistent with our findings of significantly increased mRNA expression for each gene [5-HT2AR, 20% increase, $t_{(10)} = 1.849$, $P = 0.09$; PLC β1, 30% increase, $t_{(10)} = 2.87$, $P < 0.02$; RGS4, no increase, $t_{(10)} = 0.2683$, $P = 0.79$] (Fig. S2).

Chronic Ketanserin Treatment Reduces DOI Induction of Head Twitching in MIA Offspring. 5-HT2AR is a treatment target for many psychiatric diseases, particularly major depression and schizophrenia (32–34). Injection of the 5-HT2AR antagonist ketanserin in the PFC specifically inhibits DOI-induced head twitch behavior (16). Moreover, postnatal exposure to stress increases 5-HT2R and elevates sensitivity to DOI, and chronic ketanserin in adulthood prevents enhanced anxiety (35) and restores some of the DOI-induced gene expression changes in the PFC (29). We find that ketanserin treatment for a week reduces DOI-induced head twitching in MIA offspring (Fig. 1*B*) [pairwise multiple comparison for ketanserin/saline treatment, $F_{(1, 34)} = 8.787$, $P < 0.01$; for DOI/saline treatment, $F_{(1, 34)} = 266.250$, $P < 0.001$; for MIA treatment, $F_{(1, 34)} = 0.0180$, $P = 0.894$; post hoc test for DOI-induced head twitch response after ketanserin treatment, $P < 0.001$ for MIA versus controls]. In contrast, 5-HT2AR blockade has no effect on DOI-induced head twitching in control offspring (post hoc test, $P = 0.71$). The effect of ketanserin treatment on DOI-induced head twitching is not due to acute blockade of 5-HT2AR, as the drug is cleared from the organism by the time of behavioral testing (36). Compared with nontreated animals, the head twitch response to DOI is significantly higher in animals that underwent daily handling and injections of ketanserin or saline for a week (Fig. 2*A*). This can be explained by the fact that repeated stress can increase 5HT-2AR levels in the PFC (37).

Because 5-HT2AR plays a crucial role in schizophrenia, we also checked the levels of 5-HT, its endogenous ligand, in whole blood and the PFC of MIA offspring. Although there may be a slight decrease in 5-HT in blood (1.29 ± 0.67 and 1.84 ± 0.51 ng/mg protein for MIA and control offspring, respectively) and PFC (3.52 ± 1.19 and 4.73 ± 0.27 ng/mg protein for MIA and control offspring, respectively), these differences do not reach

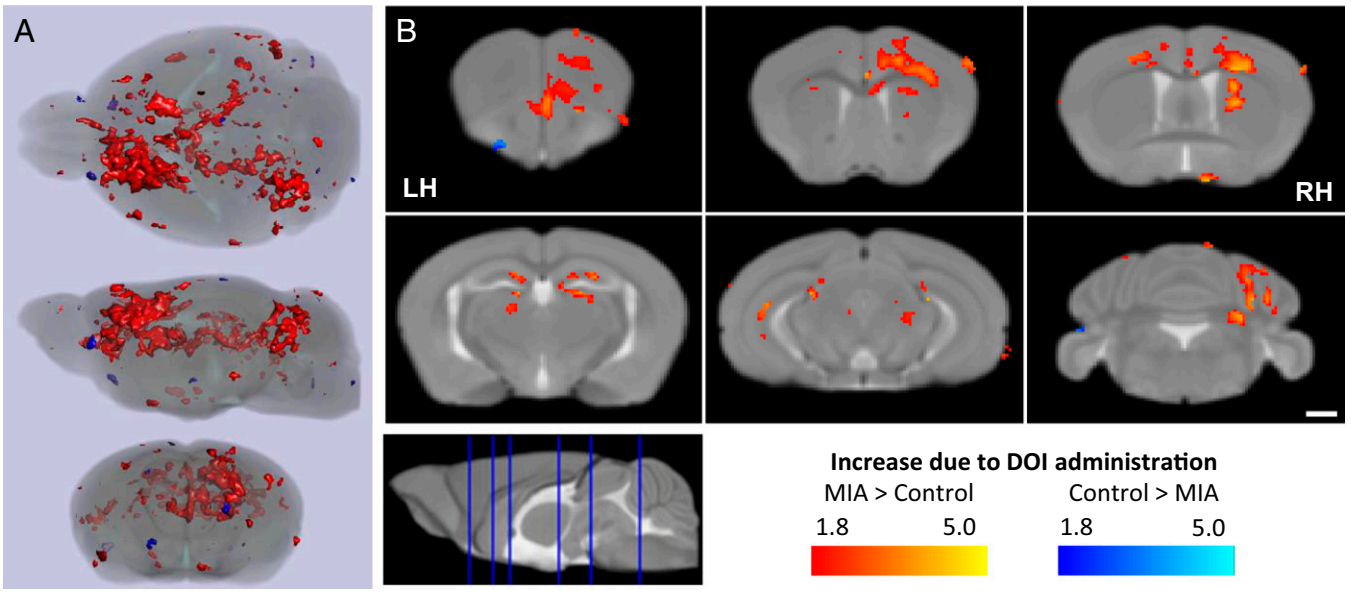

Fig. 6. DOI induces greater MEMRI signal increase in MIA versus control offspring. Significant group-wide comparison of signal increase due to DOI administration between MIA and control mice identifies areas of increase (red) and decrease (blue) of MEMRI signal between the groups. (*A*) Semitransparent renderings of the study-specific MDT and SPM overlays are displayed in axial, sagittal, and coronal profiles. (*B*) Specific coronal slices from the study-specific MDT display the SPM overlays, with significance reached at $P < 0.05$ [$t_{(11)} = 1.81$; $n = 6$ per group]. Only voxels identified demonstrating significant interaction effects between drug and group are included in this figure. (Scale bar, 1 mm.) LH, left hemisphere; RH, right hemisphere.

statistical significance [$t_{(10)} = 0.665$, $P = 0.26$ and $t_{(10)} = 0.631$, $P = 0.27$ for blood and brain samples, respectively].

Discussion

The principal findings of this study are as follows: (*i*) in addition to deficient prepulse inhibition (PPI) of the startle response (Fig. S3), MIA results in offspring with a schizophrenia-like behavioral trait, namely, an elevated sensitivity to the hallucinogenic drug DOI; (*ii*) MIA offspring display greater DOI-induced egr-1, COX-2, and BDNF expression in the PFC; (*iii*) MEMRI reveals that DOI stimulates the frontal, primary motor, and somatosensory cortices as well as caudate putamen and thalamic

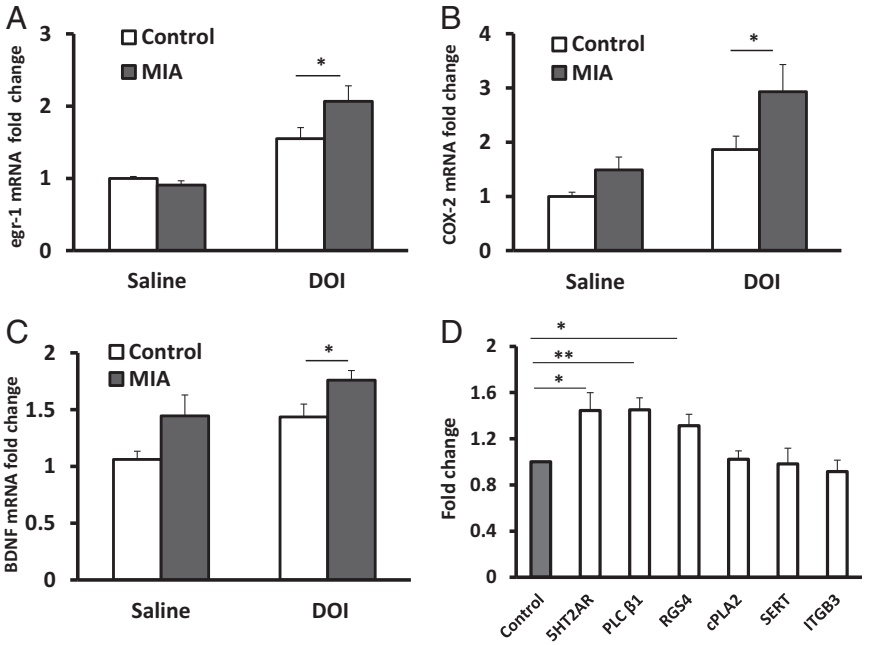

Fig. 7. MIA offspring display enhanced molecular responses to DOI in the PFC. The DOI induction of egr-1 (*A*), COX-2 (*B*), and BDNF (*C*) activation is greater than in MIA than control PFC (n = 9–14 from four litters per group, $^*P < 0.05$). (*D*) Compared with controls, MIA offspring display higher expression of 5-HT2AR, PLC β1, and RGS4 mRNA in the PFC (n = 10–12 from four litters per group, $^*P < 0.05$ and $^{**}P < 0.005$). No differences between the experimental groups are seen for cPLA2, SERT, and ITGB3. The level of expression of each molecule of interest is normalized to beta-actin. Results are compared with the control group and expressed as fold-change ± SEM.

nuclei; (*iv*) Mn^{2+} uptake is significantly higher in all of these areas in MIA offspring compared with control offspring; (*v*) the PTN is the area of the brain activated by DOI in MIA offspring only; (*vi*) differences in DOI-induced Mn^{2+} accumulation and IEG expression can be explained by the increased levels of 5-HT2AR, PLC β1, and RGS4 in the PFC of MIA offspring; (*vii*) alterations in 5-HT2ARs are not due to changes in the levels of serotonin, SERT, or ITGB3; and (*viii*) chronic treatment with the 5-HT2AR antagonist ketanserin reduces DOI induction of head twitching in MIA offspring.

Multiple genetic and environmental factors can contribute to the etiology of schizophrenia (38). We and others have previously reported that the MIA mouse model yields offspring with schizophrenia-like behaviors (30, 39–43). Moreover, another environmental factor that can contribute to the onset of schizophrenia is hallucinogenic drug abuse (3). LSD, DOI, and psilocybin can induce schizophrenia-like psychosis in healthy human subjects (3, 4, 44–46), and in the case of psilocybin, the effect can be blocked by ketanserin. Furthermore, these drugs induce schizophrenia-like traits in animals such as a PPI deficit (47, 48) and stereotypic head twitches (16, 17, 49). Here, we combined these two factors, MIA and an acute injection of hallucinogenic drug DOI, and found that MIA offspring display stronger DOI-induced behavioral responses and greater brain activity as measured both by IEG induction and MEMRI. Elevated sensitivity to DOI and up-regulation of *egr-1* in the PFC was also reported previously for offspring born to influenza-infected or poly(I:C)-injected pregnant mice (30, 31). In addition, these mice also display a decreased density of metabotropic glutamate 2 receptors (mGluR2s) in the PFC. 5-HT2AR and mGluR2 can be expressed as a receptor heterocomplex in the mouse and human brain, which may represent a new target for antipsychotic therapies (50).

To characterize neuronal activation elicited by DOI administration, we used an MEMRI approach using awake, freely moving animals. Compared with earlier published approaches, where MEMRI was used to analyze the action of pharmacological agents (9), the present method is noninvasive and allows study of Mn^{2+} incorporation under a variety of behavioral situations. We found that DOI stimulates Mn^{2+} uptake in the frontal, primary motor, and somatosensory cortices as well as the caudate putamen, midbrain, and thalamus (Fig. 5, *Right* and Table S1). Signal enhancement in the motor and somatosensory cortices can be explained by increased locomotion activity, rearing, and grooming. Altogether, our MEMRI data, positron emission tomography (PET), and fMRI experiments in healthy human subjects with another 5HT-2AR agonist psilocybin (51, 52) identify the PFC and thalamus as key brain regions mediating the effects of hallucinogens. Moreover, compared with control offspring, MIA offspring display significantly higher DOI-induced brain activity in most of the described areas (Fig. 6 and Table S2). Interestingly, MIA offspring, but not the controls, display DOI-induced Mn^{2+} accumulation in the PTN, one of the intralaminar nuclei of the dorsal thalamus that is known to play a role in the pathogenesis of the visual and auditory hallucinations (53, 54).

We focus our study on PFC, as it plays an important role in cognition, mood, anxiety, and sensory gating. Clinical, neuropsychological, and neuroimaging studies demonstrate PFC dysfunction in schizophrenia (55–57). Because this area of the brain receives dense serotonergic innervation, abnormalities of the serotonergic pathway have been proposed to contribute to the pathophysiology of schizophrenia (58, 59). 5-HTRs are highly expressed in human and rodent PFC and regulate PFC excitability (60–62). We focused on 5-HT2AR and its signaling pathway, as this receptor is a direct target of DOI (17). Compared with controls, MIA offspring display an elevated level of 5-HT2AR in the PFC, which can explain the deficit of sensory gating and greater DOI-induced schizophrenia-like behavior and brain activity in these animals. Increased 5-HT2AR in the PFC was also reported for other rodent models that exhibit high sensitivity to DOI (29–31). Moreover, similar observations were made in antipsychotic-free schizophrenic subjects (28). Increased 5-HT2AR in MIA offspring may be explained by a higher density of pyramidal neurons that express this receptor, which was shown previously for the maternal influenza mouse model (63). Another possible cause for 5-HT2AR elevation in MIA offspring is that MIA may lead to activation of DNA methyltransferase 1 (DNMT1), which hypermethylates the 5-HT2AR promoter and, as a result, increases 5-HT2AR expression. There is a positive correlation between DNMT1 expression and the level of allele C-specific methylation of the 5-HT2AR promoter in the temporal cortex of schizophrenia patients, and this can significantly affect expression of the receptor (64).

5-HT2AR is a $G\alpha_q$ protein-coupled receptor, and it activates multiple signaling pathways including the PLC β1 and PLA_2 cascades and activation of Ca^{2+} channels (65, 66). Moreover, deletion of the G_q gene results in the lack of DOI-induced head twitches (67). The complexity of 5-HT2AR signaling may help to explain the paradox of why structurally similar 5-HT2AR ligands differ in their hallucinogenic effects. We find that DOI activation of 5-HT2AR results in an increased expression of egr-1, COX-2, and BDNF mRNAs. Compared with controls, MIA offspring demonstrate higher levels of all three targets.

Egr-1 is an IEG whose expression can be activated by PLC β1. Thus, the higher induction of *egr-1* expression by DOI in MIA offspring compared with controls may be due to the elevated PLC β1 level in the MIA offspring. Contradictory findings on PLC β1 expression in the PFC of schizophrenia patients have been reported (68, 69). This discrepancy may be due to differences in the state of the disease or therapy in these patient cohorts. Interestingly, a recent study reported an elevated rate of *PLC* β1 gene deletions in schizophrenia patients (70). In addition, compared with controls, MIA offspring display an elevated RGS4 level in the PFC. RGS4 is a modulator of G protein and Ca^{2+} signaling and is highly expressed in the PFC. RGS4 suppresses Gα subunit activity by promoting hydrolysis of GTP and by antagonizing the regulation of Gα effectors (71). The elevated levels of RGS4 in the PFC of MIA offspring may represent an adaptive mechanism to reduce 5-HT2AR–mediated $G\alpha_q$ overactivity, which causes activation of PLC β1 and Ca^{2+} signaling pathways. Although there are decreased levels of RGS4 in schizophrenia patients (72), RGS4 knockout mice do not display relevant behavioral abnormalities (73).

Expression of *COX-2* and *BDNF* is very rapidly induced by neuronal activity (74, 75). Moreover, DOI increases expression of these genes in the rat parietal cortex (25, 27). We confirmed this in the mouse PFC. MIA offspring display not only higher basal *COX-2* and *BDNF* expression than controls but also an increased response to DOI. Increased COX-2 and BDNF levels are also found in schizophrenia patients (76, 77).

Because MIA offspring display increased 5-HT2AR levels, we also checked other components of the serotonergic system such as 5-HT, as well as SERT and ITGB3, which are involved in 5-HT transport. We found that MIA has no effect on basal 5-HT content in the PFC. Similar findings were reported for the MIA mouse model earlier (39, 78). Moreover, MIA does not change basal expression of SERT and ITGB3. Therefore, alterations in the 5-HT2ARs but not in the level of serotonin, SERT, or ITGB in MIA offspring contribute to schizophrenia-related traits such as high sensitivity to hallucinogenic drugs.

Although many atypical antipsychotic drugs typically used to treat schizophrenia are relatively potent 5-HT2AR antagonists, they also display properties of antagonists/inverse agonists at other (particularly dopaminergic, histaminergic, and/or adrenergic) neurotransmitter receptors. Therefore, the search for highly selective antagonists for 5-HT2AR is needed (79). To

date, there are a few studies that show that 5-HT2AR antagonist ketanserin inhibits psilocybin-induced acute hallucinatory states and a psychosis-like syndrome in humans (4, 45, 46). Ketanserin was also used previously to chronically block 5-HT2AR in a rat model of psychiatric vulnerability that displays high sensitivity to DOI and an increased level of 5-HT2AR in the PFC (29, 35). Those animals displayed increased DOI-induced heat twitching response and altered PFC transcriptome, components of which overlap with gene expression changes seen with DOI stimulation. We found that systemic treatment with ketanserin reduces DOI-induced head twitching in MIA offspring. Although ketanserin treatment has the effect on MIA offspring, it does not influence a baseline response in the control group. A possible explanation may be that MIA mice display elevated 5-HT2R function that is mediating the response to DOI, and chronical blockade of 5-HT2AR predominantly modulates its expression in MIA mice.

In conclusion, here we model a positive symptom of schizophrenia, hallucination-like activity, in a mouse model of an environmental risk factor of schizophrenia, MIA. MIA offspring display an enhanced susceptibility to the psychomimetic actions of DOI and demonstrate elevated DOI-induced brain activity as measured by IEG induction and MEMRI. The increased 5-HT2AR expression and the ability of ketanserin to reduce DOI-induced head twitching in MIA offspring suggest 5-HT2AR as a potential therapeutic target for schizophrenia. Moreover, understanding the mechanism of hallucinogen actions on the brain may help identify new treatment options and should increase the awareness of the dangers of abuse of such drugs.

Materials and Methods

Animals. Pregnant female C57BL/6J mice (Charles River) were obtained from the California Institute of Technology breeding facility and were housed under standard laboratory conditions. All animal protocols were approved by the Institutional Animal Care and Use Committee of the California Institute of Technology. On E10.5, pregnant females were weighed and randomly assigned to poly(I:C) or saline groups. The offspring were weaned at 3 wk of age, and males were caged in groups of two to four. All behavioral tests were conducted between 900 and 1700 h during the light phase of the circadian cycle. Only male offspring were tested to avoid the effects of ovarian hormones on female behavior.

Administration of Poly(I:C). One group of mice was given 5 mg/kg poly(I:C) (potassium salt; Sigma) or saline i.p. on E10.5, 12.5, and 14.5, as was reported previously (1). The manufacturer supplies poly(I:C) at 10% of the total weight of the salt, and the dosage was based on the weight of poly(I:C) itself.

DOI-Induced Stereotyped Behavior. Eight- to 10-wk old control and MIA offspring received (±)DOI hydrochloride (1 or 2 mg/kg, i.p.) (Sigma) or saline. Twenty-four hours before injection, the animals were single housed and moved to a quiet testing room with red light to decrease the effects of external stimuli on the sensory cortex. Behavioral responses to the drug or vehicle were recorded in the home cage for 30 min after the injection. Head twitches were defined as rapid radial movements of the head and were counted by an experimenter blind to the treatment group.

Quantitative RT-PCR. Quantitative RT-PCR (qRT-PCR) was performed to determine the influence of MIA on 5-HT2AR, PLC β1, $cPLA_2$, RGS4, SERT, and ITGB3 mRNA expression in unstimulated animals. In a separate experiment, we analyzed how DOI stimulates mRNA expression of IEGs such as egr-1, COX-2, and BDNF in the PFC of MIA and control offspring. IEG activation was measured after 1 h of stimulation with DOI (1 mg/kg).

To collect brain samples, mice were anesthetized using Nembutal and then decapitated. Brains were removed and washed in ice-cold, RNase-free saline for 1–2 min. The PFC was dissected, homogenized in TRIzol (15 mg tissue per 600 μL), frozen in dry ice, and stored at −80 °C until processed for total RNA isolation. Total RNA was extracted following the manufacturer's protocol (Qiagen), reverse-transcribed using an iScript cDNA Synthesis Kit (Bio-Rad), and subjected to qPCR using FastStart SYBR Green Master (Roche Applied Science) and the Applied Biosystems 7300 Real-Time PCR System (Applied Biosystems). Quantification was determined using the Ct method as described in the manufacturer's protocol (Applied Biosystems). Data from all groups were normalized to β-actin. Each sample was run in triplicate. Results were compared with the control group and expressed as fold-change ± SEM. The primers were chosen to span an intron to avoid the detection of any contamination of genomic DNA. Table S3 lists the primers used.

Blockade of the 5-HT2AR. To block 5-HT2ARs, control and MIA animals were treated with the 5-HT2AR antagonist ketanserin (Sigma) (2 mg/kg) or saline i.p. daily for 7 d. The half-life of ketanserin in plasma is about 15 h (36). Two days after the last injection, when the drug was totally cleared, the animals were assessed for behavioral responses to DOI (1 mg/kg). This approach allows analysis of effects of ketanserin on gene expression, in the absence of acute 5-HT2AR blockade.

Determination of 5-HT Content. Mouse blood was drawn by cardiac puncture using citrate–dextrose solution (Sigma). Platelets were lysed by addition of buffer [20 mM Tris·HCl, pH 7.8, 1.25 mM EDTA, 120 mM NaCl, 0.5% Nonidet P-40, 0.5% Triton, Complete Protease Inhibitor Mixture, EDTA-free and PhosSTOP-Phosphatase Inhibitor Mixture (Roche Applied Science)]. The 5-HT content in mouse whole blood was measured using a 5-HT ELISA Kit (Eagle Biosciences, Inc.). The amount of 5-HT was normalized to 1 mg of total protein. The protein concentration was measured using CB-X Protein Assay (G-Biosciences, A Geno Technology, Inc.).

Statistical Analysis. Statistical analysis for behavioral data and qRT-PCR was performed using Prism 4.0b (Graphpad) and SigmaPlot 10 (Systat Software). Experiments with two groups were analyzed using the unpaired Student *t* test. Experiments with two variable factors were subjected to two-way ANOVA, followed by a Bonferroni post hoc test. Experiments with three variable factors were subjected to three-way ANOVA, followed by a Bonferroni post hoc test.

MEMRI. Fig. 4 illustrates the timeline of the MEMRI protocol. Mice were imaged 1 wk before administration of Mn^{2+} to acquire a baseline image. On the first day of the experiment all animals received $MnCl_2$ (40 mmole/kg body weight) i.p. After $MnCl_2$ injection the animals were moved to a room with red light. Twenty-four hours following $MnCl_2$ injection, mice were imaged to measure the basal level of Mn^{2+} uptake in the brain. After imaging, the animals were returned to the room with red light. After 1 h of recovery from anesthesia, the animals were injected i.p. with DOI (2 mg/kg) or saline twice, 1 h apart. Then, 1 h after the last injection, the animals were imaged again to measure DOI-induced Mn^{2+} uptake in the brain.

An 11.7 T 89 mm vertical bore Bruker BioSpin Avance DRX500 scanner (Bruker BioSpin) equipped with a Micro 2.5 gradient system was used to acquire all mouse brain images with a 35 mm linear birdcage radio frequency (RF) coil. During imaging each animal was anesthetized with 2% (vol/vol) isoflurane, and its head was secured in a Teflon stereotaxic unit within the RF coil to minimize movement and to aid in reproducible placement. Temperature and respiration were continuously monitored during data acquisition, with the temperature controlled at 37 °C and respiration maintained at 100–120/min.

Similar to previous MEMRI studies (80, 81), we used a 3D rapid acquisition with relaxation enhancement (RARE) imaging sequence (82) with a RARE factor of 4 and the following parameters: 4 averages; repetition time/effective echo time, 250 ms/12 ms; matrix size,160 × 128 × 88; field of view, 16 mm × 12.8 mm × 8.8 mm—yielding 100 μm isotropic voxels with a 46-min scan time. MR images were skull-stripped using MIPAV (http://mipav.cit.nih.gov/clickwrap.php). After skull-stripping, each image was scaled to the mode of its intensity histogram. Inaccuracies were corrected by manual revision of the masks in either image processing tool. The average time point images from the 24 and 27 h time points were used to generate an MDT. All images were warped to this MDT and then blurred with 0.3 mm Gaussian kernel (Automatic Image Registration) (83). Signal intensity difference (SID) images were generated by subtracting the 24 h time point image from the 27 h time point image for each animal.

To identify DOI-induced brain responses in control and MIA offspring, we applied SPM analysis, a voxel-based approach, which is generally used to measure functional brain activity and identify regionally specific responses to experimental factors (9, 12, 84). The images were assessed using a 2 × 2 ANOVA with the SID as the dependent variable and drug (DOI or vehicle) and MIA treatment [poly(I:C) or saline] as the independent variables. The voxels that demonstrate a statistically significant interaction between dependent variables were identified. Corrections for multiple comparison effects were calculated using Alphasim (http://afni.nimh.nih.gov/pub/dist/doc/program_help/AlphaSim.html), and significance was considered reached at $P < 0.0001$ with a minimum cluster size of 36 voxels corresponding

to $\alpha = 0.01$, $n = 6$ per group. Approximately 7% (39,670) of nonzero voxels in the MDT were identified as statistically significant, which corresponds to less than 2.3% of all voxels in the image field of view. DOI-induced activity patterns were represented using statistical parametric maps of F values derived from MEMRI images. Voxels that demonstrated a statistically significant interaction between the dependent variables were then investigated to determine the origin of this interaction. The SID images for the MIA and control groups were assessed to identify if the signal changes due to drug administration were different. Student t test for independent means in a group-wise manner was applied, and statistical significance was reached at $P < 0.05$ [$t_{(11)} = 1.81$, $n = 6$ per group]. Parametric maps of voxels with statistically significant changes in intensity were created to display the results and to correlate increases with underlying anatomy (Allen Brain Atlas, http://mouse.brain-map.org/). The areas of parametric maps that did not correspond to known anatomical regions were automatically excluded from the data analysis. Although all MEMRI analyses presented were corrected for multiple comparison effects, there were select brain regions (hippocampus and cerebellum) with a strong MR signal contrast at their borders. It is difficult to determine if this is truly activation or an artifact of the warping analysis approach. The signal in the white matter is the result of Mn^{2+} transport, as it is known that Mn^{2+} not only accumulates in active neurons, but it is also transported along axons and it can be observed in several synapses along a circuit (10, 85). Our manuscript focuses on prefrontal, motor, and sensory cortices and thalamus as primary sites of DOI effect, and thus, the identified border-rich regions of the hippocampus and cerebellum as well as white matter are not target regions of interest. Additional experiments should be conducted to validate whether identified sites exhibit direct activation or distal accumulation or Mn^{2+} via axonal transport, but are out of the scope of this paper.

ACKNOWLEDGMENTS. The authors acknowledge the kind assistance of A. Perles-Barbacaru, E. Hsiao, J. Ko, W. Wu, and J. Zinnanti in reviewing the manuscript; L. Rodriguez for support and administrative assistance; M. Moore for technical help; E. Bearer for manuscript discussion; L. Sandoval, R. Sauza, and J. Rodriguez for maintaining the animals; and K. Piatkov for primer design. This research was supported by a National Institute of Mental Health Exceptional Unconventional Research Enabling Knowledge Acceleration award (MH086781; to P.H.P.), an Elizabeth Ross Fellowship for the Study of Mental Illness (to N.V.M.), a National Institute of Biomedical Imaging and Bioengineering award (R01 EB000993; to J.J.G. and R.E.J.), and a National Institute of Neurological Disorders and Stroke award (NS062184; to J.J.G. and R.E.J.).

1. Malkova NV, Yu CZ, Hsiao EY, Moore MJ, Patterson PH (2012) Maternal immune activation yields offspring displaying mouse versions of the three core symptoms of autism. *Brain Behav Immun* 26(4):607–616.
2. Meyer U, Feldon J, Dammann O (2011) Schizophrenia and autism: Both shared and disorder-specific pathogenesis via perinatal inflammation? *Pediatr Res* 69(5 Pt 2): 26R–33R.
3. Paparelli A, Di Forti M, Morrison PD, Murray RM (2011) Drug-induced psychosis: How to avoid star gazing in schizophrenia research by looking at more obvious sources of light. *Front Behav Neurosci* 5:1.
4. Vollenweider FX, Vollenweider-Scherpenhuyzen MF, Bäbler A, Vogel H, Hell D (1998) Psilocybin induces schizophrenia-like psychosis in humans via a serotonin-2 agonist action. *Neuroreport* 9(17):3897–3902.
5. Turner WM, Tsuang MT (1990) Impact of substance abuse on the course and outcome of schizophrenia. *Schizophr Bull* 16(1):87–95.
6. Patterson PH (2009) Immune involvement in schizophrenia and autism: Etiology, pathology and animal models. *Behav Brain Res* 204(2):313–321.
7. Meyer U, Feldon J (2012) To poly(I:C) or not to poly(I:C): Advancing preclinical schizophrenia research through the use of prenatal immune activation models. *Neuropharmacology* 62(3):1308–1321.
8. Romero E, et al. (2007) Neurobehavioral and immunological consequences of prenatal immune activation in rats. Influence of antipsychotics. *Neuropsychopharmacology* 32(8): 1791–1804.
9. Lu H, et al. (2007) Cocaine-induced brain activation detected by dynamic manganese-enhanced magnetic resonance imaging (MEMRI). *Proc Natl Acad Sci USA* 104(7): 2489–2494.
10. Van der Linden A, Van Meir V, Tindemans I, Verhoye M, Balthazart J (2004) Applications of manganese-enhanced magnetic resonance imaging (MEMRI) to image brain plasticity in song birds. *NMR Biomed* 17(8):602–612.
11. Yu X, Wadghiri YZ, Sanes DH, Turnbull DH (2005) In vivo auditory brain mapping in mice with Mn-enhanced MRI. *Nat Neurosci* 8(7):961–968.
12. Yu X, et al. (2008) Statistical mapping of sound-evoked activity in the mouse auditory midbrain using Mn-enhanced MRI. *Neuroimage* 39(1):223–230.
13. Corne SJ, Pickering RW (1967) A possible correlation between drug-induced hallucinations in man and a behavioural response in mice. *Psychopharmacology (Berl)* 11(1): 65–78.
14. González-Maeso J, et al. (2007) Hallucinogens recruit specific cortical 5-HT(2A) receptor-mediated signaling pathways to affect behavior. *Neuron* 53(3):439–452.
15. Nakagawasai O, et al. (2004) Monoamine oxidase and head-twitch response in mice. Mechanisms of alpha-methylated substrate derivatives. *Neurotoxicology* 25(1-2): 223–232.
16. Willins DL, Meltzer HY (1997) Direct injection of 5-HT2A receptor agonists into the medial prefrontal cortex produces a head-twitch response in rats. *J Pharmacol Exp Ther* 282(2):699–706.
17. González-Maeso J, et al. (2003) Transcriptome fingerprints distinguish hallucinogenic and nonhallucinogenic 5-hydroxytryptamine 2A receptor agonist effects in mouse somatosensory cortex. *J Neurosci* 23(26):8836–8843.
18. Perles-Barbacaru TA, Procissi D, Demyanenko AV, Jacobs RE (2012) Quantitative pharmacologic MRI in mice. *NMR Biomed* 25(4):498–505.
19. McKune CM, Watts SW (2001) Characterization of the serotonin receptor mediating contraction in the mouse thoracic aorta and signal pathway coupling. *J Pharmacol Exp Ther* 297(1):88–95.
20. Nagatomo T, Rashid M, Abul Muntasir H, Komiyama T (2004) Functions of 5-HT2A receptor and its antagonists in the cardiovascular system. *Pharmacol Ther* 104(1): 59–81.
21. Pautler RG, Koretsky AP (2002) Tracing odor-induced activation in the olfactory bulbs of mice using manganese-enhanced magnetic resonance imaging. *Neuroimage* 16(2): 441–448.
22. Silva AC, Lee JH, Aoki I, Koretsky AP (2004) Manganese-enhanced magnetic resonance imaging (MEMRI): Methodological and practical considerations. *NMR Biomed* 17(8): 532–543.
23. Zwingmann C, Leibfritz D, Hazell AS (2003) Energy metabolism in astrocytes and neurons treated with manganese: Relation among cell-specific energy failure, glucose metabolism, and intercellular trafficking using multinuclear NMR-spectroscopic analysis. *J Cereb Blood Flow Metab* 23(6):756–771.
24. Amargós-Bosch M, et al. (2004) Co-expression and in vivo interaction of serotonin1A and serotonin2A receptors in pyramidal neurons of prefrontal cortex. *Cereb Cortex* 14(3):281–299.
25. Mackowiak M, et al. (2002) DOI, an agonist of 5-HT2A/2C serotonin receptor, alters the expression of cyclooxygenase-2 in the rat parietal cortex. *J Physiol Pharmacol* 53(3):395–407.
26. Angelucci F, Brenè S, Mathé AA (2005) BDNF in schizophrenia, depression and corresponding animal models. *Mol Psychiatry* 10(4):345–352.
27. Vaidya VA, Marek GJ, Aghajanian GK, Duman RS (1997) 5-HT2A receptor-mediated regulation of brain-derived neurotrophic factor mRNA in the hippocampus and the neocortex. *J Neurosci* 17(8):2785–2795.
28. Muguruza C, et al. (2013) Dysregulated 5-HT(2A) receptor binding in postmortem frontal cortex of schizophrenic subjects. *Eur Neuropsychopharmacol* 23(8):852–864.
29. Benekareddy M, Goodfellow NM, Lambe EK, Vaidya VA (2010) Enhanced function of prefrontal serotonin 5-HT(2) receptors in a rat model of psychiatric vulnerability. *J Neurosci* 30(36):12138–12150.
30. Moreno JL, et al. (2011) Maternal influenza viral infection causes schizophrenia-like alterations of 5-HT_2A and mGlu_2 receptors in the adult offspring. *J Neurosci* 31(5): 1863–1872.
31. Holloway T, et al. (2013) Prenatal stress induces schizophrenia-like alterations of serotonin 2A and metabotropic glutamate 2 receptors in the adult offspring: Role of maternal immune system. *J Neurosci* 33(3):1088–1098.
32. Meltzer HY, Li Z, Kaneda Y, Ichikawa J (2003) Serotonin receptors: Their key role in drugs to treat schizophrenia. *Prog Neuropsychopharmacol Biol Psychiatry* 27(7): 1159–1172.
33. Rasmussen H, et al. (2011) Serotonin2A receptor blockade and clinical effect in first-episode schizophrenia patients treated with quetiapine. *Psychopharmacology (Berl)* 213(2-3):583–592.
34. Meltzer HY, Massey BW, Horiguchi M (2012) Serotonin receptors as targets for drugs useful to treat psychosis and cognitive impairment in schizophrenia. *Curr Pharm Biotechnol* 13(8):1572–1586.
35. Benekareddy M, Vadodaria KC, Nair AR, Vaidya VA (2011) Postnatal serotonin type 2 receptor blockade prevents the emergence of anxiety behavior, dysregulated stress-induced immediate early gene responses, and specific transcriptional changes that arise following early life stress. *Biol Psychiatry* 70(11):1024–1032.
36. Trenk D, Mosler A, Kirch W, Meinertz T, Jähnchen E (1983) Pharmacokinetics and pharmacodynamics of the 5-HT2 receptor antagonist ketanserin in man. *J Cardiovasc Pharmacol* 5(6):1034–1039.
37. Dwivedi Y, Mondal AC, Payappagoudar GV, Rizavi HS (2005) Differential regulation of serotonin (5HT)2A receptor mRNA and protein levels after single and repeated stress in rat brain: Role in learned helplessness behavior. *Neuropharmacology* 48(2): 204–214.
38. Brown AS (2012) Epidemiologic studies of exposure to prenatal infection and risk of schizophrenia and autism. *Dev Neurobiol* 72(10):1272–1276.
39. Bitanihirwe BK, Peleg-Raibstein D, Mouttet F, Feldon J, Meyer U (2010) Late prenatal immune activation in mice leads to behavioral and neurochemical abnormalities relevant to the negative symptoms of schizophrenia. *Neuropsychopharmacology* 35(12):2462–2478.
40. Meyer U, Feldon J, Fatemi SH (2009) In-vivo rodent models for the experimental investigation of prenatal immune activation effects in neurodevelopmental brain disorders. *Neurosci Biobehav Rev* 33(7):1061–1079.
41. Shi L, Fatemi SH, Sidwell RW, Patterson PH (2003) Maternal influenza infection causes marked behavioral and pharmacological changes in the offspring. *J Neurosci* 23(1): 297–302.
42. Smith SE, Li J, Garbett K, Mirnics K, Patterson PH (2007) Maternal immune activation alters fetal brain development through interleukin-6. *J Neurosci* 27(40):10695–10702.

43. Zuckerman L, Weiner I (2005) Maternal immune activation leads to behavioral and pharmacological changes in the adult offspring. *J Psychiatr Res* 39(3):311–323.
44. Vardy MM, Kay SR (1983) LSD psychosis or LSD-induced schizophrenia? A multimethod inquiry. *Arch Gen Psychiatry* 40(8):877–883.
45. Quednow BB, Kometer M, Geyer MA, Vollenweider FX (2012) Psilocybin-induced deficits in automatic and controlled inhibition are attenuated by ketanserin in healthy human volunteers. *Neuropsychopharmacology* 37(3):630–640.
46. Kometer M, Schmidt A, Jäncke L, Vollenweider FX (2013) Activation of serotonin 2A receptors underlies the psilocybin-induced effects on α oscillations, N170 visual-evoked potentials, and visual hallucinations. *J Neurosci* 33(25):10544–10551.
47. Farid M, Martinez ZA, Geyer MA, Swerdlow NR (2000) Regulation of sensorimotor gating of the startle reflex by serotonin 2A receptors. Ontogeny and strain differences. *Neuropsychopharmacology* 23(6):623–632.
48. Halberstadt AL, Geyer MA (2010) LSD but not lisuride disrupts prepulse inhibition in rats by activating the 5-HT(2A) receptor. *Psychopharmacology (Berl)* 208(2):179–189.
49. Hanks JB, González-Maeso J (2013) Animal models of serotonergic psychedelics. *ACS Chem Neurosci* 4(1):33–42.
50. Moreno JL, Sealfon SC, González-Maeso J (2009) Group II metabotropic glutamate receptors and schizophrenia. *Cell Mol Life Sci* 66(23):3777–3785.
51. Carhart-Harris RL, et al. (2012) Neural correlates of the psychedelic state as determined by fMRI studies with psilocybin. *Proc Natl Acad Sci USA* 109(6):2138–2143.
52. Vollenweider FX, et al. (1997) Positron emission tomography and fluorodeoxyglucose studies of metabolic hyperfrontality and psychopathology in the psilocybin model of psychosis. *Neuropsychopharmacology* 16(5):357–372.
53. Delgado MG, Bogousslavsky J (2013) 'Distorteidolias'—Fantastic perceptive distortion. A new, pure dorsomedial thalamic syndrome. *Eur Neurol* 70(1-2):6–9.
54. Boes APS, Caviness V, Fox M (2013) The neuroanatomy of peduncular hallucinosis: A case series and lesion overlap analysis. *Neurology* 80(Meeting Abstracts 1):S18.004.
55. Barch DM, Ceaser A (2012) Cognition in schizophrenia: Core psychological and neural mechanisms. *Trends Cogn Sci* 16(1):27–34.
56. Buchsbaum MS, Hazlett EA (1998) Positron emission tomography studies of abnormal glucose metabolism in schizophrenia. *Schizophr Bull* 24(3):343–364.
57. Sapara A, et al. (2007) Prefrontal cortex and insight in schizophrenia: A volumetric MRI study. *Schizophr Res* 89(1-3):22–34.
58. Abi-Dargham A (2007) Alterations of serotonin transmission in schizophrenia. *Int Rev Neurobiol* 78:133–164.
59. Iqbal N, van Praag HM (1995) The role of serotonin in schizophrenia. *Eur Neuropsychopharmacol* 5(Suppl):11–23.
60. Lambe EK, Fillman SG, Webster MJ, Shannon Weickert C (2011) Serotonin receptor expression in human prefrontal cortex: Balancing excitation and inhibition across postnatal development. *PLoS ONE* 6(7):e22799.
61. Puig MV (2011) Serotonergic modulation of the prefrontal cortex: From neurons to brain waves. *Psychiatric Disorders—Worldwide Advances*, ed Uehara T (InTech, Croatia), pp 3–22.
62. Hawrylycz MJ, et al. (2012) An anatomically comprehensive atlas of the adult human brain transcriptome. *Nature* 489(7416):391–399.
63. Fatemi SH, et al. (2002) Prenatal viral infection leads to pyramidal cell atrophy and macrocephaly in adulthood: Implications for genesis of autism and schizophrenia. *Cell Mol Neurobiol* 22(1):25–33.
64. Polesskaya OO, Aston C, Sokolov BP (2006) Allele C-specific methylation of the 5-HT2A receptor gene: Evidence for correlation with its expression and expression of DNA methylase DNMT1. *J Neurosci Res* 83(3):362–373.
65. Millan MJ, Marin P, Bockaert J, Mannoury la Cour C (2008) Signaling at G-protein-coupled serotonin receptors: Recent advances and future research directions. *Trends Pharmacol Sci* 29(9):454–464.
66. Weinstein H (2005) Hallucinogen actions on 5-HT receptors reveal distinct mechanisms of activation and signaling by G protein-coupled receptors. *AAPS J* 7(4): E871–E884.
67. Garcia EE, Smith RL, Sanders-Bush E (2007) Role of G(q) protein in behavioral effects of the hallucinogenic drug 1-(2,5-dimethoxy-4-iodophenyl)-2-aminopropane. *Neuropharmacology* 52(8):1671–1677.
68. Lin XH, Kitamura N, Hashimoto T, Shirakawa O, Maeda K (1999) Opposite changes in phosphoinositide-specific phospholipase C immunoreactivity in the left prefrontal and superior temporal cortex of patients with chronic schizophrenia. *Biol Psychiatry* 46(12):1665–1671.
69. Udawela M, Scarr E, Hannan AJ, Thomas EA, Dean B (2011) Phospholipase C beta 1 expression in the dorsolateral prefrontal cortex from patients with schizophrenia at different stages of illness. *Aust N Z J Psychiatry* 45(2):140–147.
70. Lo Vasco VR, Cardinale G, Polonia P (2012) Deletion of PLCB1 gene in schizophrenia-affected patients. *J Cell Mol Med* 16(4):844–851.
71. Hollinger S, Hepler JR (2002) Cellular regulation of RGS proteins: Modulators and integrators of G protein signaling. *Pharmacol Rev* 54(3):527–559.
72. Mirnics K, Middleton FA, Stanwood GD, Lewis DA, Levitt P (2001) Disease-specific changes in regulator of G-protein signaling 4 (RGS4) expression in schizophrenia. *Mol Psychiatry* 6(3):293–301.
73. Grillet N, et al. (2005) Generation and characterization of Rgs4 mutant mice. *Mol Cell Biol* 25(10):4221–4228.
74. Lauterborn JC, et al. (1996) Differential effects of protein synthesis inhibition on the activity-dependent expression of BDNF transcripts: Evidence for immediate-early gene responses from specific promoters. *J Neurosci* 16(23):7428–7436.
75. Yermakova A, O'Banion MK (2000) Cyclooxygenases in the central nervous system: Implications for treatment of neurological disorders. *Curr Pharm Des* 6(17): 1755–1776.
76. Takahashi M, et al. (2000) Abnormal expression of brain-derived neurotrophic factor and its receptor in the corticolimbic system of schizophrenic patients. *Mol Psychiatry* 5(3):293–300.
77. Tang B, Capitao C, Dean B, Thomas EA (2012) Differential age- and disease-related effects on the expression of genes related to the arachidonic acid signaling pathway in schizophrenia. *Psychiatry Res* 196(2-3):201–206.
78. Winter C, et al. (2009) Prenatal immune activation leads to multiple changes in basal neurotransmitter levels in the adult brain: Implications for brain disorders of neurodevelopmental origin such as schizophrenia. *Int J Neuropsychopharmacol* 12(4): 513–524.
79. Ebdrup BH, Rasmussen H, Arnt J, Glenthøj B (2011) Serotonin 2A receptor antagonists for treatment of schizophrenia. *Expert Opin Investig Drugs* 20(9):1211–1223.
80. Gallagher JJ, et al. (2013) Altered reward circuitry in the norepinephrine transporter knockout mouse. *PLoS ONE* 8(3):e57597.
81. Gallagher JJ, Zhang X, Ziomek GJ, Jacobs RE, Bearer EL (2012) Deficits in axonal transport in hippocampal-based circuitry and the visual pathway in APP knock-out animals witnessed by manganese enhanced MRI. *Neuroimage* 60(3):1856–1866.
82. Hennig J, Nauerth A, Friedburg H (1986) RARE imaging: A fast imaging method for clinical MR. *Magn Reson Med* 3(6):823–833.
83. Woods RP, Grafton ST, Watson JD, Sicotte NL, Mazziotta JC (1998) Automated image registration: II. Intersubject validation of linear and nonlinear models. *J Comput Assist Tomogr* 22(1):153–165.
84. Friston KJ (2003) Statistical parametric mapping. *Statistical Parametric Mapping: The Analysis of Functional Brain Images*, eds Penny WD, Friston KJ, Ashburner JT, Kiebel SJ, Nichols TE (Academic, Burlington, MA), pp 10–31.
85. Pautler RG (2004) In vivo, trans-synaptic tract-tracing utilizing manganese-enhanced magnetic resonance imaging (MEMRI). *NMR Biomed* 17(8):595–601.